IEEE Access
Multidisciplinary | Rapid Review | Open Access Journal

Received June 12, 2020, accepted June 25, 2020, date of publication July 2, 2020, date of current version July 17, 2020.

Digital Object Identifier 10.1109/ACCESS.2020.3006495

Rapid Vitality Estimation and Prediction of Corn Seeds Based on Spectra and Images Using Deep Learning and Hyperspectral Imaging Techniques

LEI PANG[1], SEN MEN[2,3], LEI YAN[1], (Member, IEEE), AND JIANG XIAO[1]

[1]School of Technology, Beijing Forestry University, Beijing 100083, China
[2]College of Robotics, Beijing Union University, Beijing 100020, China
[3]Beijing Engineering Research Center of Smart Mechanical Innovation Design Service, Beijing Union University, Beijing 100020, China

Corresponding author: Lei Yan (mark_yanlei@bjfu.edu.cn)

This work was supported in part by the National Natural Science Foundation of China under Grant 31770769, in part by the National Key Research and Development Program of China under Grant 2017YFC0504403, in part by the Fundamental Research Funds for the Central Universities under Grant 2015ZCQ-GX-03, and in part by the General Program of Science and Technology Development Project of Beijing Municipal Education Commission of China under Grant KM201911417008.

ABSTRACT Highly viable seeds are of great significance for agricultural development, and the traditional corn seed vigor detection method is time-consuming and laborious. In this paper, the spectral and image information of hyperspectral imaging was used, and a distinction between seed vigor detection and prediction was proposed. The potential of hyperspectral imaging technology and convolutional neural networks (CNNs) to identify and predict maize seed vitality was evaluated. The hyperspectral information in 10 hours before the germination of four vigor level seeds (144 samples each) was collected. A support vector machine, extreme learning machine, and one-dimensional convolutional neural network (1DCNN) were used to model the spectral data set, comparing the effects of multidimensional scattering correction and principal component analysis. 1DCNN performed best on the original spectral data, reaching an accurate recognition of 90.11%. According to the spectral changes of the seed germination, the first three hours of data were selected for prediction, which had higher recognition accuracy than the test set. The image-based 2DCNN model achieved 99.96% accurate recognition at a fast convergence speed. By differentiating the spectra and image information, the various CNN models can achieve accurate detection and prediction, providing a framework to advance research on seed germination.

INDEX TERMS Convolutional neural network, hyperspectral image, image, seed vitality, spectrum.

I. INTRODUCTION

Seed vigor is a complex physiological characteristic, which includes seed germination and emergence rate, seedling growth potential, plant stress resistance, and production potential, and is an important indicator of seed quality [1]. Highly viable seeds are beneficial to increase emergence rates and crop yields and to have a strong resistance to adverse conditions. Poor storage conditions, such as high moisture content (>14%) or high temperature (>25 °C), or physical damage during post-harvest mechanical processing are reasons for the loss of vitality of corn seeds. Seed germination, a major determinant of the productivity of any crop [2], [3], refers to a series of orderly physiological and morphogenetic processes from seed imbibition. The seeds begin to exhale vigorously when they absorb water and expand, so many enzymes in the seeds are synthesized or activated, including proteases, amylases, and lipases.

Corn (*Zea mays* L.) is currently one of the most widely used food crops. It has high nutritional value and is characterized by a variety of uses from feed to high-tech industries. Corn seeds often lose their vigor after harvest due to environmental conditions or improper storage. It is necessary to conduct seed vitality testing to maximize corn production. According to the provisions of the International Seed Inspection Association (ISTA) [4], corn seed vitality can be tested using standard germination tests, accelerated aging tests [5], conductivity tests, tetrazolium staining [6], and other methods. These methods

The associate editor coordinating the review of this manuscript and approving it for publication was Gustavo Callico.

have some shortcomings, such as subjectivity, invasiveness, low specificity, long time-consuming, and low accuracy [7].

The emergence of modern spectroscopy technology has promoted the process of rapid and non-destructive testing of seed vigor. For example, Fourier near-infrared spectroscopy (FT-NIR) and Raman methods are based on vibrational spectroscopy to take advantage of the differences in biochemical composition between aged and normal seeds [8], [9]. These methods have also proved to be meaningful in the discrimination of other crop varieties [10] and the detection of internal components [11]. However, due to the characteristics of spot scanning, it is impossible to obtain all the information needed for full evaluations.

Hyperspectral imaging allows a model to combine the spectrum with the image where hundreds of single-channel black and white (grayscale) images (each image representing a spectral wavelength band) are stacked on top of each other to produce a hypercube [12]. It has become one of the most powerful and useful technologies for agricultural and forestry crop quality and safety testing, such as in variety or damage identification [13], [14], component detection [15], and seed vigor identification.

The purpose of this study was to use hyperspectral imaging combined with convolutional neural networks (CNN) in vigor detection and vitality prediction of corn seeds. The specific contributions are as follows:

(1) Advance research on the change of spectra during the germination of seeds, and propose a new way for detection and prediction of vigor.
(2) Analyze the spectral change characteristics of seeds with different vitality levels in the first 10 hours of germination.
(3) Compare the performance of traditional modeling and 1DCNN model on the spectral data set, and study the effects of multidimensional scattering correction (MSC) and principal component analysis (PCA).
(4) Select the optimal time to make predictions based on the prediction ability under the spectral vitality detection model.
(5) Establish a 2DCNN recognition model on the image data and compare its performance with 1DCNN.

II. RELATED WORK

When hyperspectral imaging technology is used for seed quality and safety testing, it mainly involves the following aspects: seed classification, vitality detection, damage detection, internal composition determination, and cleanliness detection [16]. There were many kinds of research objects included, but research on wheat, rice, corn, and other major crop seeds has obvious practical applications. The following studies are some that have introduced hyperspectral technology for the classification, vigor, and composition-related detection of corn seeds.

Jia *et al.* studied identification methods of coated maize seed varieties and established the identification models of four corn varieties using support vector machine (SVM), similar soft independent modeling, and bionic pattern recognition, with a high recognition rate of 97.5% [17]. Accurate identification of 17 varieties of maize seeds was feasible using vector fusion of spectral features and image features (morphology and texture) [18]. Cui *et al.* explored a method for corn haploid seed screening and verified it with partial least squares regression (PLSR) [19].

Moisture content is one important indicator to evaluate seed quality because it directly affects storage time and seed germination rate. Zhang and Guo [20], based on visible/near-infrared and near-infrared hyperspectral imaging technology, achieved accurate non-destructive testing of corn seed moisture content. A PLSR model was established and different spectral preprocessing methods were compared. Among them, S-G smoothing was a suitable pre-processing method.

Other studies have demonstrated the potential of hyperspectral imaging combined with pattern recognition algorithms to develop seed vitality and vigor prediction models. For 300 microwave high temperature-treated samples and 300 untreated samples based on hyperspectral activity measurement at 1000–2500nm [21], the highest spectral classification rate obtained by SVM in was up to 100%. The same post-aging vitality approach was carried out on yellow, white, and purple corn seeds [7]. Using partial least squares discriminant analysis (PLS-DA) for classification, the accuracy of the training set and test set exceeded 95%.

The processing and feature extraction of large amounts of hyperspectral data requires appropriate methods. Deep learning (DL) is effective and popular for handling complex classification problems in large-capacity data [22]. CNN is one of the most popular deep learning models, employing local receptive fields, weight sharing, and subsampling [23], [24]. In the hyperspectral field, CNN has been used to classify one-dimensional spectral data, two-dimensional images, and three-dimensional hyperspectral remote sensing data. Using PLS-DA, SVM, and CNN to establish a discriminant model for the identification of narrow-leaved oleaster geographical origins, the classification accuracy exceeded 90% [25]. Nie *et al.* [26] used the same three models to distinguish hybrid okra seeds and hybrid loofah seeds. The discriminant analysis model based on DCNN was the most stable.

When summarizing the existing methods in the previous literature, several deficiencies are noted. First, in most of the previous studies, only multi-band spectral features or simple image features were used to establish the discriminant model. Three varieties of corn seeds were identified based on hyperspectral information at 380 bands (400–1000nm) [27]. Orrillo *et al.* used 159 band spectra 900–1710 nm to identify papaya seeds mixed with black pepper [28]. When the hyperspectral imaging technology is used to detect seed vitality, the changes in spectra and other information during seed germination are generally ignored, and the method of combining image information and deep learning had not been fully applied. This paper actively studied the spectra of the seed germination process and applied CNN to establish the recognition models based on spectra and images.

TABLE 1. Germination of corn seeds at various vitality levels.

Seed sample	Number of samples	Viable seeds	Unviable seeds	Germination rate (%)
Normal	144	136	8	94.4
Aging for three days	144	105	39	72.9
Aging for six days	144	82	62	57.0
Aging for nine days	144	34	110	23.6
Total	576	357	219	62.0

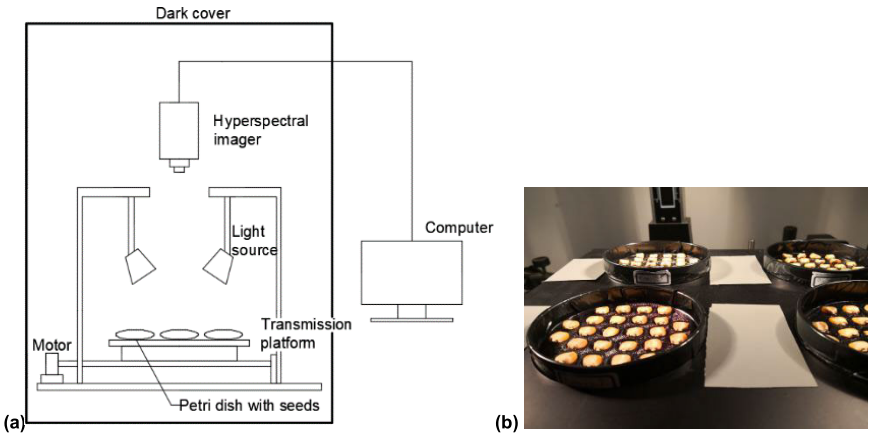

FIGURE 1. (a) Hyperspectral data collection system; (b) some corn samples in the experiment.

III. MATERIALS AND METHODS

A. CORN SEED SAMPLES

The corn variety used in this experiment was Huanong 101. The experimental seeds were purchased at Beijing Seed Market. After preliminary screening, the seeds were divided into four groups for artificially accelerated aging. One group did not undergo any treatment (normal seeds), and the remaining three groups were heat-treated in an artificial aging box at 45 °C and relative humidity of 98% [43]. After aging for 3, 6, or 9 days, the seeds were removed and returned to room temperature. Then, 144 samples of uniform size were randomly selected from each of the four groups for subsequent experiments (a total of 576 samples).

B. STANDARD GERMINATION TEST

For verification, all corn seeds were tested for germination following ISTA rules. The samples were placed on sterilized germination paper and then stored in an incubator without light at 25 °C and 65% relative humidity (except for the time of data collection). During germination, all seeds were visually inspected daily for seven days. After seven days, seeds that had sprouted with shoots longer than 1 cm were counted as viable seeds [29]. The final number of germinated seeds is given in Table 1.

C. HYPERSPECTRAL IMAGING SYSTEM

A multi-channel hyperspectral imaging system was used for image acquisition and spectral measurement of corn seeds, which was employed for the first 10 h of the above germination (at intervals of 0.5 h). The data acquisition system consisted of several units (Fig.1(a)). A model SOC710VP hyperspectral imager (Surface Optics Corp., San Diego, CA, USA) has a built-in scanning design and a 12-bit dynamic range array imaging CCD. The image resolution was 520 × 696 pixels and the spectral resolution 4.6875 nm (128 spectral bands from 370.2 to 1042.3 nm). The lighting unit consisted of two 250W halogen lamps (OSRAM GCA; Sylvania, Gloucester, MA, USA), illuminating at an angle of 45°. The mobile platform allowed the relative position of the experimental samples at each time point to not significantly change. Fig. 1(b) is the placement of some samples in the experiment, with the endosperm-containing side facing up and the reverse side facing down.

D. HYPERSPECTRAL DATA ACQUISITION

The acquired images contain significant noise and the images need to be corrected to reduce or eliminate the effects of light source changes and dark current. The camera lens was completely covered to obtain a black reference (I_D), and a white Teflon tile was used with a reflectivity close to 100% as a white reference (I_W). The original image (I_R) was corrected by Equation 1 to get a corrected image (I).

$$I = (I_R - I_D)/(I_W - I_D) \tag{1}$$

The complete seed served as the region of interest (ROI). To reduce the negative effects of surface scattering, the spectra at both ends were intercepted and 115 wavelength points in the wavelength range of 440.6 to 1003.7 nm were retained. Due to the baseline drift of corn seeds, there was still noise interference in the data, so the spectral data was pre-processed

with MSC. MSC is a commonly used data processing method for multi-wavelength calibration modeling [30], which can correct the spectrum through baseline shifts and offset corrections to improve the original signal-to-noise ratio.

E. MULTIVARIATE DATA ANALYSIS

1) SUPPORT VECTOR MACHINE

SVM was proposed in 1964 and developed rapidly after the 1990s yielding a series of improved and extended algorithms. It has applications for pattern recognition problems in various fields, including portrait recognition, text classification, handwritten character recognition, and bioinformatics [31]–[34]. The hinge loss function is used to calculate the empirical risk and a regularization term is added to the solution system to optimize the structural risk. It realizes nonlinear classification through the kernel method [35]. The Radial Basis Function kernel (also called the Gaussian kernel) and its corresponding mapping function maps the sample space to an infinite dimensional space.

2) EXTREME LEARNING MACHINE

An extreme learning machine (ELM) is a type of machine learning system or method based on a feed-forward neural network, which is suitable for supervised and unsupervised learning problems [36]. Its characteristic is that the weights of the hidden layer nodes are randomly or artificially given and do not need to be updated [37]. The standard ELM uses a single layer feed-forward neuron network (SLFN) structure. SLFN consists of an input layer, a hidden layer, and output layer. The output function of the hidden layer is represented by:

$$f_L = \sum \beta_i h_i(x) = h(x)\beta \tag{2}$$

where x is the input of the neural network, β is the output weight, and $h(x)$ is a feature map or excitation function to map the input layer data from its original space to the ELM feature space.

3) DEEP CONVOLUTIONAL NEURAL NETWORK

CNN is a type of feed-forward neural network that includes convolution calculations and has a deep structure [38]. It can represent learning and classify the input information according to its hierarchical structure. CNN is an efficient, high-performance, hyperspectral data analysis method due to its ability to assist automatic feature learning [39]. A typical CNN contains five modules: input, convolutional layer, pooling layer, fully connected layer, and output. CNN integrates feature learning, feature extraction, dimensionality reduction, and final classification into one system [40]. Similar to other neural network algorithms, since the gradient descent algorithm is used for learning, the input features of the CNN need to be standardized.

The input layer of CNN can process multi-dimensional data. In this paper, 1DCNN and 2DCNN were used to classify and identify the spectra and image information of corn seeds, respectively. Their structure diagram is shown in Fig. 2. IDCNN consisted of four double-layer convolutional layers with 16, 32, 64, and 128 filters, with a kernel size of 3, a stride of 1, and no padding. The MaxPooling layer was configured with a pool size of 2, a stride of 2, and no padding. The three fully connected layers are 512, 128, and 4 in size. Use dropout alleviates overfitting and BatchNormalization is used to carry out the batch standardization process. 2DCNN contained only two convolutional layers and three fully connected layers, and thus was much simpler than 1DCNN. Most of the parameters have been given in Fig. 2, and the filling method and step size were consistent with 1DCNN. In the 2DCNN model, the image under each band of each corn seed was cropped to 55 * 55.

F. SOFTWARE TOOLS

Matlab R2019a (The MathWorks, Natick, MA, USA) was used to achieve spectral extraction, preprocessing, and corn

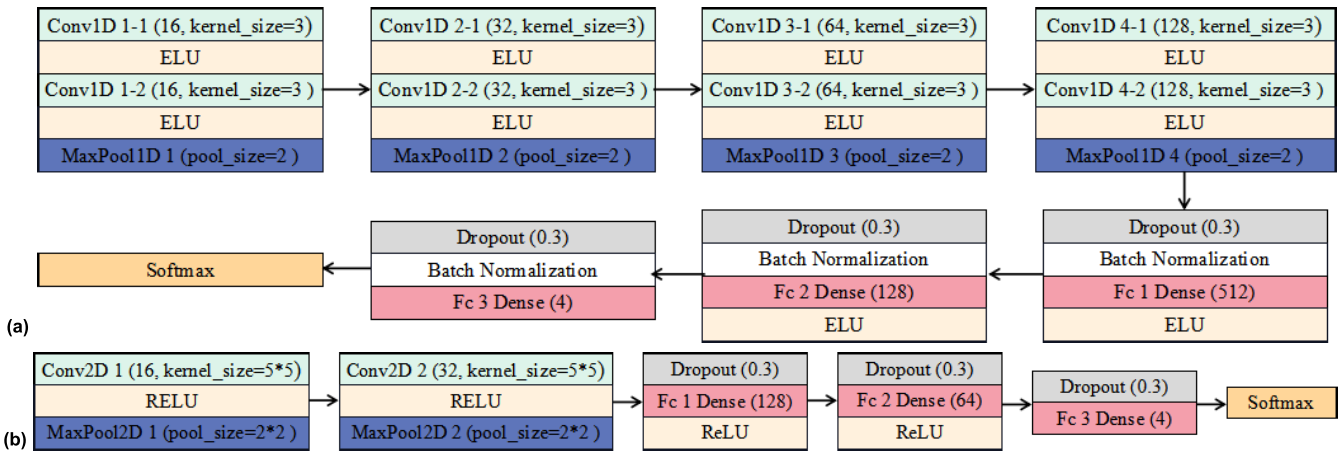

FIGURE 2. Structure flow chart of (a) 1DCNN and (b) 2DCNN.

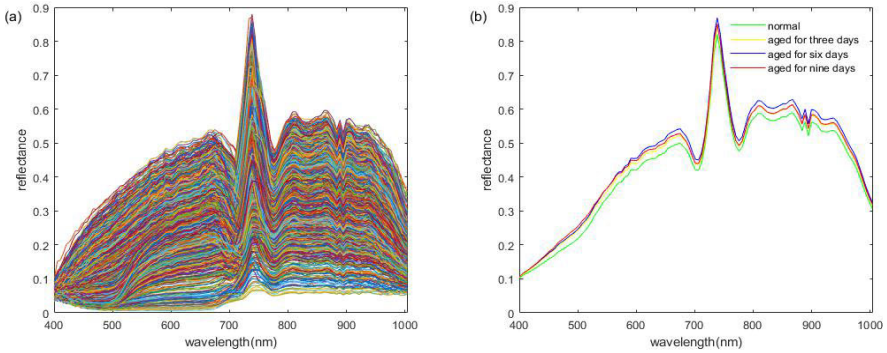

FIGURE 3. The unprocessed spectrum of corn seeds of four vitality levels during germination: (a) all samples; (b) average spectra of four vitality levels.

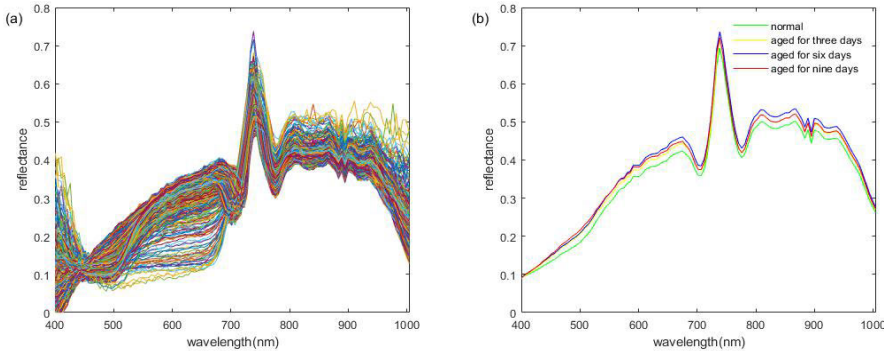

FIGURE 4. The spectra of varying vigor corn seeds after MSC preprocessing during germination: (a) all samples; (b) mean spectra of four vigor grades.

seed image segmentation, and PCA, SVM, and ELM were also performed. The 1DCNN and 2DCNN models were built in Python 3.6 and a Tensorflow framework ran on the graphics processing unit were also performed.

IV. RESULTS AND DISCUSSION

A. SPECTRAL CHARACTERISTICS

The original and average spectra of the four vigor grade corn seeds over the wavelength range of 400–1000nm are shown in Fig. 3(a) and 3(b), respectively. Although there was much overlap in the original spectrum, the general trends of the spectral curves were quite similar. In the visible light range (400–780nm), the spectral reflectance first increases and then several obvious peaks and troughs appeared. The remaining band belonged to the short-wave near-infrared region, and the reflectivity remained relatively stable within a range and then declined. It is well known that the visible and near-infrared spectra provide chemical information about the main components containing hydrogen-containing functional groups [41]. For example, the absorption peaks at 883, 889, and 896 nm were caused by the third harmonic stretching of the O-H functional group related to water [42]. In summary, the spectral characteristic information of seeds was reflected in different characteristic bands and this characteristic information can be used to describe seed vigor.

Fig. 4(a) and Fig. 4(b) are all spectra and average spectra after MSC preprocessing. The average spectrum after pretreatment was similar to the original average spectrum, but it was found from the overall spectrum that MSC eliminated the scattering thereby obtaining a more concentrated reflection spectrum.

B. EXPLORATORY ANALYSIS AND FEATURE SELECTING USING PCA

The PCA analysis was carried out on the germination spectral information of each corn seed to explore the intuitive distinguishability of corn seeds. This work was performed on the original spectrum and the spectrum after MSC preprocessing. The first three PCs of the above two were used for analysis because their cumulative contribution rate exceeded 95% (the former was 91.72%, 5.13%, and 2.08%, the latter was 78.99%, 14.81%, and 4.06%). According to Fig. 5 (a, b, and c), in the original spectral scatter plot, the seeds of aging treatments had no obvious boundaries during the germination process which was consistent with the results of Feng *et al.* [43]. Spectral scatter plots after pretreatment (Fig. 5d, e, and f) showed better differentiation compared to the original spectrum, especially when separating normal seed data, which meant that the divergence of hyperspectral data between corn grains not aged and aged was greater.

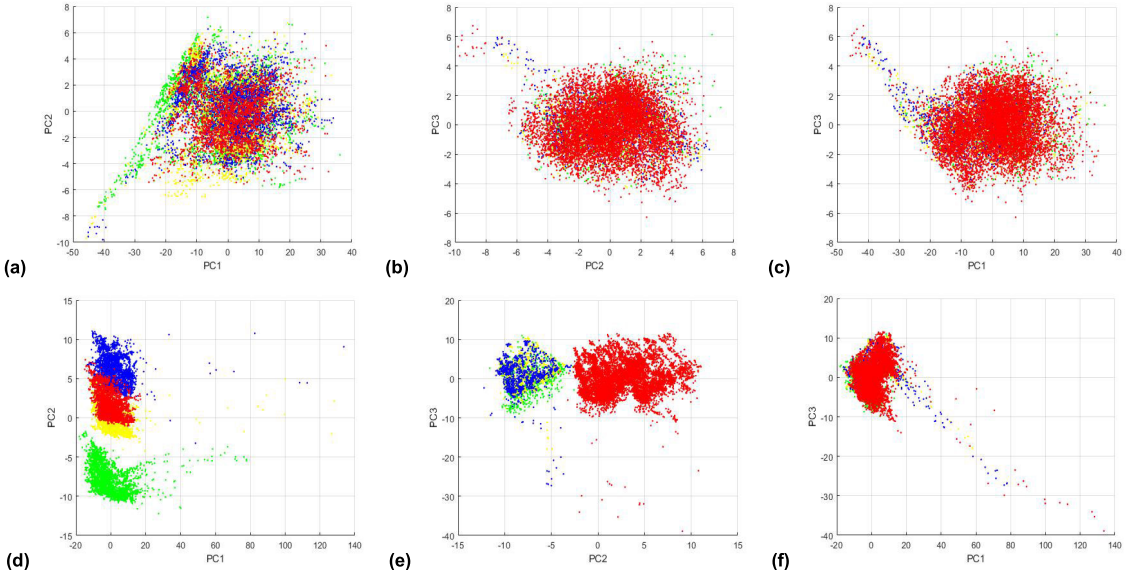

FIGURE 5. PCA score scatter plots of maize kernels under different aging duration time: (a) PC1 versus PC2 for original spectrum; (b) PC2 versus PC3 for original spectrum; (c) PC1 versus PC3 for original spectrum; (d) PC1 versus PC2 for processed spectrum; (e) PC2 versus PC3 for processed spectrum; (f) PC1 versus PC3 for processed spectrum (Scattered color representation is consistent with Fig. 4).

Although the variance of the variables was maximized after PCA dimensionality reduction, the linear separability of different categories was not achieved.

Another function of PCA was the feature dimensionality reduction to extract the optimal band. This operation also targeted the original spectrum and the pre-processed spectrum. The weight coefficient of each feature in the first two PCs was determined according to the projection matrix during the PCA transformation. Finally, multiple local maxima were identified in each PC, that is, the location of each peak was selected as the optimal band. The number of specific bands and corresponding wavelength values are given in Table 2.

TABLE 2. Results of the optimal band determined by PCA.

Data set	Number of variables	Specific band value (nm)
Raw spectrum	17	431.1, 508.0, 539.0, 657.1, 674.9, 701.3, 706.6, 722.5, 749.1, 754.5, 759.8, 775.8, 813.3, 834.8, 867.2, 943.3, 987.2
Spectrum after MSC preprocessing	15	405.7, 487.4, 502.9, 544.2, 606.6, 632.8, 664.4, 701.3, 738.5, 781.2, 818.7, 834.8, 883.5, 943.4, 976.2

C. SPECTRAL ANALYSIS DURING GERMINATION

The average spectrum change of corn seeds with different vitality levels within 10 h of germination is shown in Fig. 6. The overall spectral reflectance of the four types of samples showed a downward trend over the entire period. The spectrum of these objects was inconsistent. For example, the spectrum of the first 2 h for normal seeds had a clear boundary with the follow-up, while the 6-day seeds were only distinguished by the first 0 h data. The internal material content of the seeds will change during the process of water absorption and germination, as energy and nutrient storage substances (e.g., starch, proteins, and lipids) are activated [44]. However, the various viable corn seeds have diverse abilities to transform or decompose substances, which lead to the differences in the spectral changes within 10 h.

To visually display and compare the changes of the corn seeds spectra with different vigor during the germination process, a curve of spectral reflectance with time was constructed using the following method. What was critical was the weight coefficient corresponding to each band in PC1 with PCA analysis ($n = 115$). Suppose A_i is the spectral matrix (144^*n) of the i-th hour, and the coefficient matrix extracted by PC1 is w (1^*n). Then the following formula can be used to get the combined reflectance value (R_{new}):

$$R_{new} = \left(\frac{(A_i * w)'}{n} \right)' \Big/ 144 \quad (i = 0, 0.5, \ldots 11) \qquad (3)$$

This is repeated with the data each time and vitality levels according to the above method, and the final curve shown in Fig. 7 is obtained. The four treatments had crossovers and overlap within 0–2h, which meant that it was not easy to distinguish among them within this period. Also, the normal seeds and the three-day aging seeds crossed at 2.5–3 h. As the germination time increased, the seed curves converge. This reflects the discrepancies in the spectral changes during germination and also provided a basis for subsequent vitality prediction.

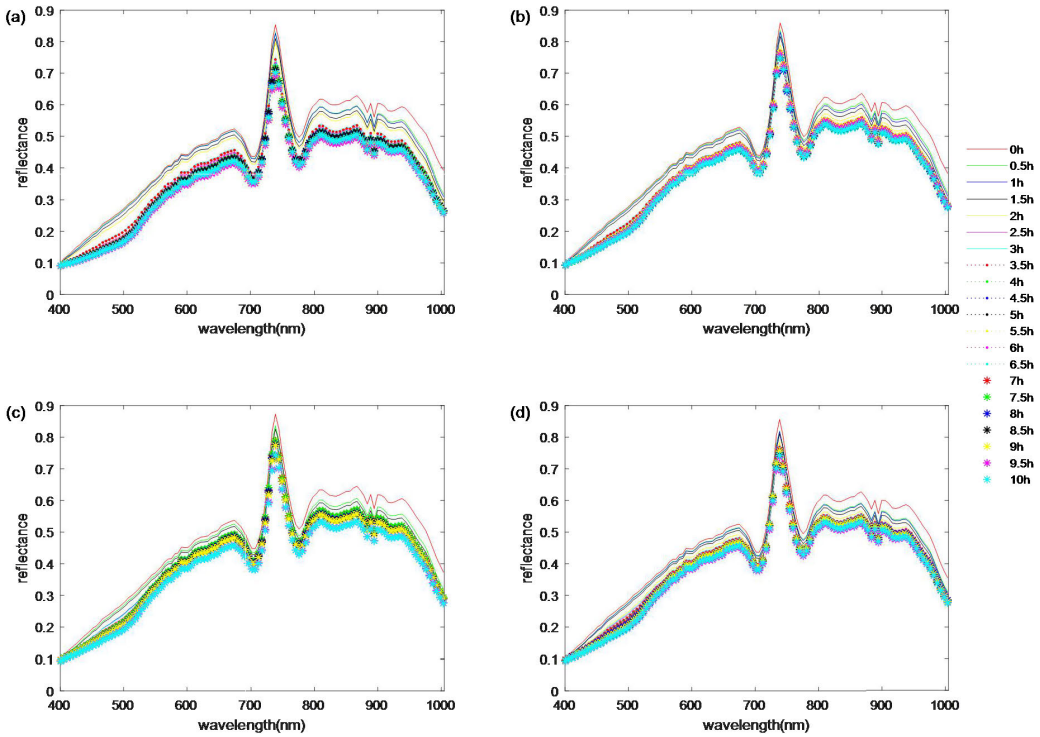

FIGURE 6. The average spectral change curve of corn seeds during germination: (a) normal; (b) aging for three days; (c) aging for six days; (d) aging for nine days.

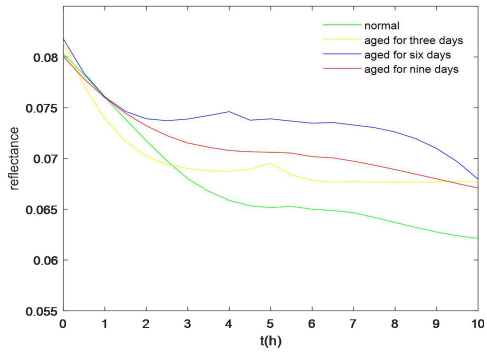

FIGURE 7. The curve of the spectral reflectance with time during 10 hours of germination.

D. VITALITY DISCRIMINATION RESULTS OF MODELS BASED ON SPECTRA

Spectral discriminant models were established by SVM, ELM, and 1DCNN on different data sets. Cross-validation was used to estimate the accuracy of the algorithm. The data were divided into four parts, and three of them were taken as training data and one as test data. The average accuracy was obtained after repeating four times as the final recognition result. Each data model identified the optimal parameters according to its data characteristics. The overall results are shown in Table 3. The ELM model was not ideal for the original spectral data; although the accuracy of the SVM training set was 99.95%, the difference between the test set and it was too large. Under the CNN model, both the training set and the test set were more than 90% accurate. Compared with the first two models, CNN was more conducive to massive data modeling and effective feature application. This was consistent with the results of chrysanthemum variety identification, in which DCNN was superior to SVM and linear regression [39].

In addition to the original spectral information, the effects of preprocessing and feature selection were analyzed. Whether it was SVM, ELM, or CNN, MSC preprocessing was an effective measure to improve accuracy. Its use not only significantly enhanced the ability of ELM to recognize different vitality corn seeds (twice the accuracy) but also achieved accurate recognition of about 99% for both SVM and CNN. Yang *et al.* [45] also showed the contribution of multiple preprocessing methods to the model performance when classifying sugar beet. The use of characteristic bands was not an effective way to improve the performance of the model; ELM was close to the original spectral model results, but SVM and 1DCNN decreased greatly. This was because although only 17 bands were used in the feature model and the calculation speed was fast, much useful information was lost. The characteristic band modeling selected by the successive projection algorithm also reduced the accuracy of SVM in the classification of hybrid okra seeds [46]. Also, the feature models of SVM and ELM performed well after the preprocessing, with 15 features reaching a similar or higher accuracy than the preprocessing model. This effect

TABLE 3. Results of corn seed vitality detection and prediction model based on spectral information.

Models	Number of bands	Vitality detection with 10 h data		Vitality prediction for the first 3 h data (%)
		Training set (%)	Testing set (%)	
Original spectrum + SVM	115	99.95	62.44	89.14
Original spectrum + ELM	115	45.39	44.87	45.39
Original spectrum +1DCNN	115	99.80	90.11	91.09
MSC + SVM	115	100	99.95	99.98
MSC + ELM	115	88.36	88.24	88.36
MSC + 1DCNN	115	99.48	98.99	99.01
Original spectrum + PCA+SVM	17	57.95	55.33	52.2
Original spectrum + PCA+ELM	17	49.90	49.62	49.89
Original spectrum + PCA+1DCNN	17	49.09	45.33	46.86
MSC +PCA+ SVM	15	99.69	99.30	99.57
MSC +PCA+ ELM	15	90.19	89.97	90.19
MSC +PCA+ 1DCNN	15	49.72	49.99	49.59

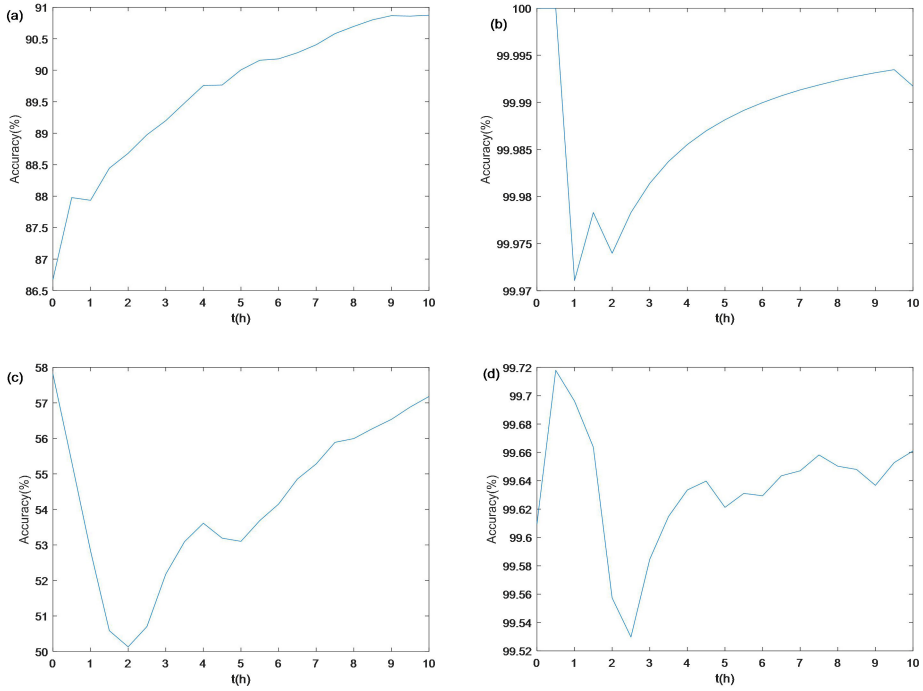

FIGURE 8. Vitality prediction results of multiple models of accumulated data within 10h: (a) SVM; (b) MSC + SVM; (c) PCA + SVM; (d) MSC + PCA + SVM.

was not possible for CNN, because the substantial reduction in data volume made CNN lose the advantage of automatically extracting features. In short, 1DCNN had a significant effect on the original high dimensional data without any processing and could extract the features of hidden layers. SVM was relatively stable because of its nonlinear mapping and the application of optimal hyperplane partitioning. Although ELM was fast, it was the single hidden layer neural network, so the accuracy of data analysis was the lowest.

Seed germination is a cumulative process, and seed internal composition is constantly changing, with the state at a given moment greatly affected by the previous stage. Based on this, the accuracy of each time point (including all data before the time point) within 10 h of germination was considered to establish a vitality prediction model. The prediction model was constructed by all methods of SVM in the vitality detection model, and the result was relatively stable and the influence of the characteristic band was not as large as that of CNN. Comparing the four prediction results shown in Figure 8, the original spectral model always maintained a trend of increasing accuracy. The other three models had a sudden drop around 2 h or 2.5 h, and then increased or remained stable. This was consistent with the pattern in Fig. 7, which was caused by the high spectral similarity and thus difficulty in distinguishing among them. Combining Fig. 7 and 8, the data from the first three hours were selected for vitality prediction (Table 3). The vitality prediction was often better for the test set, but very close to the training set result.

E. ESTABLISHMENT OF AN IMAGE-BASED CORN SEED VITALITY RECOGNITION MODEL USING 2DCNN

When establishing the 2DCNN corn seed vigor detection model, the pictures (each picture size was 55 * 55) of each seed, in each germination state, (10 h) and each band were

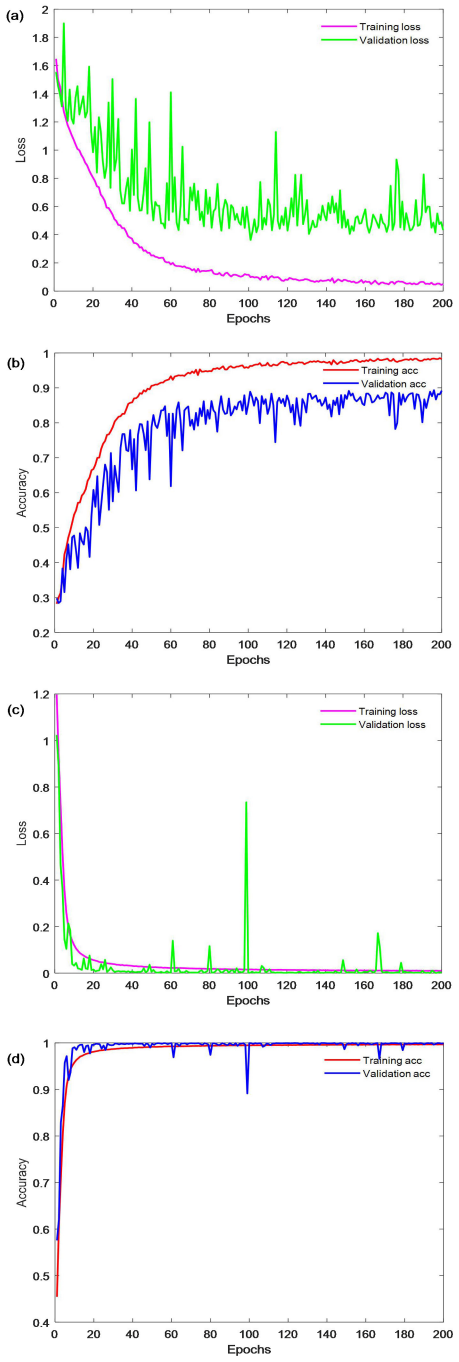

FIGURE 9. Comparison of CNN model effect between original spectrum and image information (200 iterations): (a) loss function of 1DCNN; (b) accuracy of 1DCNN; (c) loss function of 2DCNN; (d) accuracy of 2DCNN.

used. To avoid the impact of unclear pictures in some bands on the modeling, image information of 461.8–998.3 nm was applied. The training set and test set were divided 3:1 and then looped and averaged. The image recognition results based on 2DCNN are shown in Table 4, and the first three hours of image data were used for vitality prediction. Regardless of the training set, test set, or prediction, the CNN training results on the image were well within a 0.5% false-positive rate. When modeling on the corresponding pictures of the characteristic band selected by PCA, the recognition accuracy rate decreased due to a lack of data.

TABLE 4. Corn seed vitality detection and prediction based on image information.

Models	Number of corresponding bands	Vitality detection-10 h		Vitality prediction - 3 h (%)
		Training set (%)	Testing set (%)	
2DCNN	102	99.67	99.96	99.85
PCA + 2DCNN	17	68.78	68.92	68.90

When using 1DCNN and 2DCNN to establish vitality detection and prediction models for the original spectrum and the original image, the image was more powerful and did not require any preprocessing. In 200 iterations of model training, the changes were compared for the loss of function and accuracy (Fig. 9). 1DCNN performed well on the training set, but the loss function value of the test set was high, and the accuracy rate only reached about 90%, and there was an obvious oscillation. The recognition ability of the 2DCNN training set and the test set was equivalent, and the convergence speed was faster than 1DCNN. The above results showed that when combining hyperspectral and deep learning to identify corn seed vigor, the combination of 2DCNN and image was better than that of 1DCNN and spectrum. Despite a large number of pictures and the need for more running time, 2DCNN can extract more effective information from the pictures without pre-extraction.

V. CONCLUSION

Based on a combination of hyperspectral imaging technology and deep learning, this study identified and predicted corn seed vigor. Four levels of corn seeds were constructed by artificially accelerated aging, and data were collected 10 h before the germination of each. The seeds of the four grades were basically consistent in spectrum except for the difference in reflectivity, and the change trend was similar during germination. Comparing the model performance of SVM, ELM, and 1DCNN on the spectral data set, the recognition effect of 1DCNN was best on the original spectrum. After MSC preprocessing, the accuracy of each model was improved, especially SVM (from 62.44 to 99.95%), and the 1DCNN reached 98.99%. SVM and ELM remained relatively stable, while 1DCNN recognition declined due to the reduction in data quantity with PCA feature extraction. The spectrum change of seeds with different vitality levels during germination was similar, and the curve of each spectrum with time provided the possibility of short-term prediction. Based on the above data and the effect of the SVM model at each time point, the first three hours of data were selected for vitality prediction and the effect was excellent. The 2DCNN model achieved 99.96% accurate recognition of the image at a fast convergence speed. It indicated that this method was accurate in viability assessment and can achieve rapid prediction of seed vitality. The CNN model had a good recognition effect

on the hyperspectral spectrum and image data. The next steps in this research should be to distinguish more vitality levels to build comprehensive seed spectra images and a more complete database. It is also critical to establish better seed recognition models for germination based on temporal sequences.

REFERENCES

[1] R. Grasso, M. Gulino, F. Giuffrida, M. Agnello, F. Musumeci, and A. Scordino, "Non-destructive evaluation of watermelon seeds germination by using delayed luminescence," *J. Photochem. Photobiol. B, Biol.*, vol. 187, pp. 126–130, Oct. 2018.

[2] G. Kim, G.-H. Kim, S. Lohumi, J.-S. Kang, and B.-K. Cho, "Viability estimation of pepper seeds using time-resolved photothermal signal characterization," *Infr. Phys. Technol.*, vol. 67, pp. 214–221, Nov. 2014.

[3] V. Dragicevic, M. Spasic, M. Simic, Z. Dumanovic, and B. Nikolic, "Stimulative influence of germination and growth of maize seedlings originating from aged seeds by 2,4-D potencies," *Homeopathy*, vol. 102, no. 3, pp. 179–186, Jul. 2013.

[4] *International Rules for Seed Testing*, Int. Seed Test. Assoc., Bassersdorf, Switzerland, 2015, pp. 1–12.

[5] D. V. D. A. Sena, B. Universidade Federal da Paraíba, E. U. Alves, D. S. D. Medeiros, and B. U. F. da Paraíba, "Vigor tests to evaluate the physiological quality of corn seeds cv. 'Sertanejo,"' *Ciência Rural*, vol. 47, no. 3, pp. 1–7, 2017.

[6] M. Olesen, P. Nikneshan, S. Shrestha, A. Tadayyon, L. Deleuran, B. Boelt, and R. Gislum, "Viability prediction of ricinus cummunis L. Seeds using multispectral imaging," *Sensors*, vol. 15, no. 2, pp. 4592–4604, Feb. 2015.

[7] A. Ambrose, L. M. Kandpal, M. S. Kim, W.-H. Lee, and B.-K. Cho, "High speed measurement of corn seed viability using hyperspectral imaging," *Infr. Phys. Technol.*, vol. 75, pp. 173–179, Mar. 2016.

[8] A. Ambrose, S. Lohumi, W.-H. Lee, and B. K. Cho, "Comparative nondestructive measurement of corn seed viability using Fourier transform near-infrared (FT-NIR) and Raman spectroscopy," *Sens. Actuators B, Chem.*, vol. 224, pp. 500–506, Mar. 2016.

[9] D. Kusumaningrum, H. Lee, S. Lohumi, C. Mo, M. S. Kim, and B.-K. Cho, "Non-destructive technique for determining the viability of soybean (glycine max) seeds using FT-NIR spectroscopy," *J. Sci. Food Agricult.*, vol. 98, no. 5, pp. 1734–1742, Oct. 2017.

[10] G. J. Qiu, E. L. Lü, N. Wang, H. Z. Lu, F. R. Wang, and F. G. Zeng, "Cultivar classifification of single sweet corn seed using Fourier Transform Near-Infrared spectroscopy combined with discriminant analysis," *Appl. Sci.*, vol. 9, pp. 1530–1544, Apr. 2019.

[11] D. S. Ferreira, J. A. L. Pallone, and R. J. Poppi, "Direct analysis of the main chemical constituents in chenopodium Quinoa grain using Fourier transform near-infrared spectroscopy," *Food Control*, vol. 48, pp. 91–95, Feb. 2015.

[12] J. Burger and P. Geladi, "Hyperspectral NIR imaging for calibration and prediction: A comparison between image and spectrometer data for studying organic and biological samples," *Analyst*, vol. 131, pp. 1152–1160, Nov. 2006.

[13] K. Sendin, M. Manley, V. Baeten, J. A. Fernández Pierna, and P. J. Williams, "Near infrared hyperspectral imaging for white maize classification according to grading regulations," *Food Anal. Methods*, vol. 12, no. 7, pp. 1612–1624, Apr. 2019.

[14] P. Tsouvaltzisa, F. Babellahi, M. L. Amodio, and G. Colelli, "Early detection of eggplant fruit stored at chilling temperature using difffferent nondestructive optical techniques and supervise classifification algorithms," *Postharvest Biolo. Tec.*, vol. 159, pp. 111001–111009, Aug. 2020.

[15] R. Sonobe, Y. Hirono, and A. Oi, "Non-destructive detection of tea leaf Chlorophyll content using hyperspectral reflflectance and machine learning algorithms," *Plants*, vol. 9, pp. 368–386, Mar. 2020.

[16] L. Feng, S. Zhu, F. Liu, Y. He, Y. Bao, and C. Zhang, "Hyperspectral imaging for seed quality and safety inspection: A review," *Plant Methods*, vol. 15, no. 1, pp. 1–25, Dec. 2019.

[17] S. Jia, D. An, Z. Liu, J. Gu, S. Li, X. Zhang, D. Zhu, T. Guo, and Y. Yan, "Variety identification method of coated maize seeds based on near-infrared spectroscopy and chemometrics," *J. Cereal Sci.*, vol. 63, pp. 21–26, Aug. 2014.

[18] M. Huang, C. He, Q. Zhu, and J. Qin, "Maize seed variety classifification using the integration of spectral and image features combined with feature transformation based on hyperspectral imaging," *Appl. Sci.*, vol. 6, pp. 183–194, Jun. 2016.

[19] Y. Cui, W. Ge, J. Li, J. Zhang, D. An, and Y. Wei, "Screening of maize haploid kernels based on near infrared spectroscopy quantitative analysis," *Comput. Electron. Agricult.*, vol. 158, pp. 358–368, Mar. 2019.

[20] Y. Zhang and W. Guo, "Moisture content detection of maize seed based on visible/near-infrared and near-infrared hyperspectral imaging technology," *Int. J. Food Sci. Tech.*, vol. 55, pp. 631–640, Jul. 2020.

[21] C. Wakholi, L. M. Kandpal, H. Lee, H. Bae, E. Park, M. S. Kim, C. Mo, W.-H. Lee, and B.-K. Cho, "Rapid assessment of corn seed viability using short wave infrared line-scan hyperspectral imaging and chemometrics," *Sens. Actuators B, Chem.*, vol. 255, pp. 498–507, Feb. 2018.

[22] G. Farias, S. Dormido-Canto, J. Vega, G. Rattá, H. Vargas, G. Hermosilla, L. Alfaro, and A. Valencia, "Automatic feature extraction in large fusion databases by using deep learning approach," *Fusion Eng. Design*, vol. 112, pp. 979–983, Nov. 2016.

[23] J. Acquarelli, T. van Laarhoven, J. Gerretzen, T. N. Tran, L. M. C. Buydens, and E. Marchiori, "Convolutional neural networks for vibrational spectroscopic data analysis," *Analytica Chim. Acta*, vol. 954, pp. 22–31, Feb. 2017.

[24] P. Lin, X. L. Li, Y. M. Chen, and Y. He, "A deep convolutional neural network architecture for boosting image discrimination accuracy of rice species," *Food Bioprocess Technol.*, vol. 11, no. 4, pp. 765–773, Jan. 2018.

[25] P. Gao, W. Xu, T. Y. Yan, C. Zhang, X. Lv, and Y. He, "Application of near-infrared hyperspectral imaging with machine learning methods to identify geographical origins of dry narrow-leaved oleaster (elaeagnus angustifolia) fruits," *Foods*, vol. 8, pp. 620–632, Nov. 2019.

[26] P. C. Nie, J. N. Zhang, X. P. Feng, C. L. Yu, and Y. He, "Classification of hybrid seeds using near-infrared hyperspectral imaging technology combined with deep learning," *Sensor. Actuat. B-Chem.*, vol. 296, pp. 126630–126641, Oct. 2019.

[27] L. Wang, D.-W. Sun, H. Pu, and Z. Zhu, "Application of hyperspectral imaging to discriminate the variety of maize seeds," *Food Anal. Methods*, vol. 9, no. 1, pp. 225–234, May 2015.

[28] I. Orrillo, J. P. Cruz-Tirado, A. Cardenas, M. Oruna, A. Carnero, D. F. Barbin, and R. Siche, "Hyperspectral imaging as a powerful tool for identification of papaya seeds in black pepper," *Food Control*, vol. 101, pp. 45–52, Jul. 2019.

[29] *International Rules for Seed Testing*, Int. Seed Test. Assoc., Bassersdorf, Switzerland, 2008.

[30] N. Caporaso, M. B. Whitworth, and I. D. Fisk, "Protein content prediction in single wheat kernels using hyperspectral imaging," *Food Chem.*, vol. 240, pp. 32–42, Feb. 2018.

[31] A. Sun, E.-P. Lim, and W.-K. Ng, "Web classification using support vector machine," in *Proc. 4th Int. Workshop Web Inf. Data Manage. (WIDM)*, 2002, pp. 96–99.

[32] J. Qin and Z.-S. He, "A SVM face recognition method based on Gabor-featured key points," in *Proc. Int. Conf. Mach. Learn. Cybern.*, Guangzhou, China, Aug. 2005, pp. 5144–5149.

[33] P. Mishra, A. Nordon, J. Tschannerl, G. Lian, S. Redfern, and S. Marshall, "Near-infrared hyperspectral imaging for non-destructive classification of commercial tea products," *J. Food Eng.*, vol. 238, pp. 70–77, Dec. 2018.

[34] E. Byvatov and G. Schneider, "Support vector machine applications in bioinformatics," *Appl. Bioinf.*, vol. 2, pp. 67–77, Feb. 2003.

[35] W. W. Hsieh, *Machine Learning Methods in the Environmental Sciences: Neural Networks and Kernels*. Cambridge, U.K.: Cambridge Univ. Press, 2009.

[36] G. Huang, G.-B. Huang, S. Song, and K. You, "Trends in extreme learning machines: A review," *Neural Netw.*, vol. 61, pp. 32–48, Jan. 2015.

[37] G.-B. Huang, Q.-Y. Zhu, and C.-K. Siew, "Extreme learning machine: Theory and applications," *Neurocomputing*, vol. 70, nos. 1–3, pp. 489–501, Dec. 2006.

[38] Y. LeCun, B. Boser, J. S. Denker, D. Henderson, R. E. Howard, W. Hubbard, and L. D. Jackel, "Backpropagation applied to handwritten zip code recognition," *Neural Comput.*, vol. 1, no. 4, pp. 541–551, Dec. 1989.

[39] N. Wu, C. Zhang, X. Bai, X. Du, and Y. He, "Discrimination of chrysanthemum varieties using hyperspectral imaging combined with a deep convolutional neural network," *Moleclues*, vol. 23, pp. 2831–2844, Oct. 2018.

[40] N. Wu, Y. Zhang, R. Na, C. Mi, S. Zhu, Y. He, and C. Zhang, "Variety identification of oat seeds using hyperspectral imaging: Investigating the representation ability of deep convolutional neural network," *RSC Adv.*, vol. 9, no. 22, pp. 12635–12644, Apr. 2019.
[41] Y. F. Xu, H. J. Zhang, C. Zhang, P. Wu, J. B. Li, Y. Xia, and S. X. Fan, "Rapid prediction and visualization of moisture content in single cucumber (Cucumis Sativus L.) seed using hyperspectral imaging technology," *Infr. Phys. Techn.*, vol. 102, pp. 103034–103042, Sep. 2019.
[42] X. Yu, H. Lu, and D. Wu, "Development of deep learning method for predicting firmness and soluble solid content of postharvest korla fragrant pear using Vis/NIR hyperspectral reflectance imaging," *Postharvest Biol. Technol.*, vol. 141, pp. 39–49, Jul. 2018.
[43] L. Feng, S. S. Zhu, C. Zhang, Y. D. Bao, X. P. Feng, and Y. He, "Identifification of maize kernel vigor under different accelerated aging times using hyperspectral imaging," *Molecules*, vol. 23, pp. 3078–3092, Nov. 2018.
[44] J. D. Bewley, "Seed germination and dormancy," *Plant Cell*, vol. 9, no. 7, pp. 1055–1066, Jul. 1997.
[45] R. Yang, H. Tian, and J. Kan, "Classification of sugar beets based on hyperspectral and extreme learning machine methods," *Appl. Eng. Agricult.*, vol. 34, no. 6, pp. 891–897, 2018.
[46] J. N. Zhang, X. P. Feng, X. D. Liu, and Y. He, "Identifification of hybrid okra seeds based on near-infrared hyperspectral imaging technology," *Appl. Sci.*, vol. 8, no. 4, pp. 1793–1805, Oct. 2018.

LEI PANG received the B.Eng. degree from the North University of China, Taiyuan, China, in 2016. She is currently pursuing the Ph.D. degree with the School of Technology, Beijing Forestry University, Beijing, China.

Her research interests include pattern recognition, hyperspectral image processing, machine learning, and deep learning.

SEN MEN is currently a Lecturer with the College of Robotics, Beijing Union University, Beijing, China. His research interests are artificial intelligence, machine vision, seed viability assessment, and so on.

LEI YAN (Member, IEEE) is currently a Professor with the School of Technology, Beijing Forestry University, Beijing, China. His research interests include machine vision, pattern recognition, seed nondestructive testing, gait recognition, and so on.

JIANG XIAO is currently a Professor with the School of Technology, Beijing Forestry University, Beijing, China. Her research interests include wood inspection, computer vision, image process, and so on.